JOURNAL OF GUIDANCE, CONTROL, AND DYNAMICS
Vol. 18, No. 4, July–August 1995

Control of a Flexible Space Robot Executing a Docking Maneuver

Y. Chen* and L. Meirovitch†
Virginia Polytechnic Institute and State University, Blacksburg, Virginia 24061

This paper is concerned with a flexible space robot executing a docking maneuver with a target whose motion is not known a priori. The dynamical equations of the space robot are first derived by means of Lagrange's equations and then separated into two sets of equations suitable for rigid-body maneuver and vibration suppression control. For the rigid-body maneuver, on-line feedback tracking control is carried out by means of an algorithm based on Lyapunov-like methodology and using on-line measurements of the target motion. For the vibration suppression, LQR feedback control in conjunction with disturbance compensation is carried out by means of collocated sensor/actuator pairs dispersed along the flexible arms. Problems related to the digital implementation of the control algorithms, such as the bursting phenomenon and system instability, are discussed and a modified discrete-time control scheme is developed. A numerical example demonstrates the control algorithms.

I. Introduction

SOME of the functions of a space robot are to deploy or retrieve free-flying payloads and to service orbiting spacecraft. Under consideration is a robot with long flexible arms, such as in the case of the remote manipulator in the Space Shuttle. An example of such a space robot is shown in Fig. 1. The robot consists of a rigid base, two flexible arms attached to the base in series, and an end effector/payload. To carry out the mission described, the space robot must have its own control system enabling the platform to translate and rotate and its arms to rotate. In this paper, the target motion is assumed not to be known a priori, so that the control permitting the space robot to execute the docking maneuver must be based on on-line measurements.

The equations governing the behavior of space robots are nonlinear and can be expressed in the general form of the state and output equations

$$\dot{\boldsymbol{x}} = \boldsymbol{f}(\boldsymbol{x}, \boldsymbol{u}) \tag{1a}$$

$$\boldsymbol{y} = \boldsymbol{g}(\boldsymbol{x}) \tag{1b}$$

respectively, where $\boldsymbol{x}$ is the state vector, $\boldsymbol{u}$ is the control force vector, and $\boldsymbol{y}$ is the output vector, usually defined as the position and orientation variables of the end effector. The target output vector $\boldsymbol{y}_t$ is defined as the position and orientation variables of the target. We can then define the error vector as $\boldsymbol{e} = \boldsymbol{y}_t - \boldsymbol{y}$. The problem reduces to that of designing a control law $\boldsymbol{u}(t)$ so that $\boldsymbol{e}$ and its time derivative $\dot{\boldsymbol{e}}$ are driven to zero.

There are two significant differences between industrial robots in current use and space robots considered here. In the first place, industrial robots are mounted on a fixed base, whereas space robots are mounted on space platforms capable of translations and rotations. The second significant difference is that space robots must be very light, and hence very flexible, unlike industrial robots characterized by very bulky and stiff arms. The flexibility of the robot arms causes elastic vibration, which tends to affect adversely the performance of the end effector. Both a floating platform and flexibility are being considered in this paper.

In the case of space-based robots, research has been carried out on the assumption that the platform floats freely,[1–6] i.e., that there are no external forces and torques acting on the system, which implies that the system linear and angular momenta are conserved. Whereas these assumptions can be justified for a free-flying robot, they are unrealistic in the case of a space robot attempting to intercept and dock with a moving target.

The most commonly used approach to robotics can be described as follows: First, inverse kinematics is performed to obtain the desired robot configuration trajectory $\boldsymbol{q}_d(t)$ from the desired end-effector trajectory $\boldsymbol{y}_d(t)$. Then, using the system equations of motion, inverse dynamics is performed to obtain the control force realizing $\boldsymbol{q}_d(t)$. If the target motion is known a priori, the end effector's trajectory, as well as the robot trajectory, can be determined by an off-line planning algorithm. For a kinematically redundant robot, such as the one considered here, the robot redundancy can be used to achieve optimality.[7]

If the target motion is not known a priori, planning is impossible. Even when the target motion is known, it is very likely that some unexpected disturbance can cause errors. In view of this, on-line feedback control for the tracking problem, whereby the control decision is based on measurements of the current output error, appears more attractive. The technical literature on this subject is not very abundant. For tracking control, the Lyapunov stability concept appears quite useful. Wang[8] used it to design a guidance law for a spacecraft docking with another spacecraft. The two docking objects are assumed to be three-dimensional rigid bodies and to have their own control system on board. Another assumption used in Ref. 8 is that the motion of the target decays to zero with time. Recently, Novakovic[9] presented a technique using Lyapunov-like methodology for a robot tracking control problem. In this paper, the algorithm presented in Ref. 9 is adopted and modified for the tracking control of flexible space robots.

In the case of flexible space structures, maneuvering motions excite vibration of the flexible members. There are two major control schemes for flexible manipulators. The first is based on linearized models derived from the nonlinear equations of motion of the flexible manipulator on the assumption that maneuver motions are much larger than elastic motions. Such a perturbation approach was developed by Meirovitch and Quinn[10,11] and applied by Meirovitch and Kwak[12,13] to the maneuvering and control of articulated flexible spacecraft and by Modi and Chang[14] and Meirovitch and Lim[15] to the maneuvering and control of flexible robots. The second is the adaptive control,[16] which does not need dynamic models. Instead, an autoregressive moving average (ARMA) model of system identification is used.

A control law for flexible manipulators based on the Lyapunov method was proposed by Bang and Junkins.[17] It represents proportional and derivative control and includes a boundary force as a feedback force. This control scheme is valid only for problems

Received Nov. 20, 1993; revision received Sept. 23, 1994; accepted for publication Oct. 3, 1994.

*Graduate Research Assistant, Department of Engineering Science and Mechanics.

†University Distinguished Professor, Department of Engineering Science and Mechanics. Fellow AIAA.

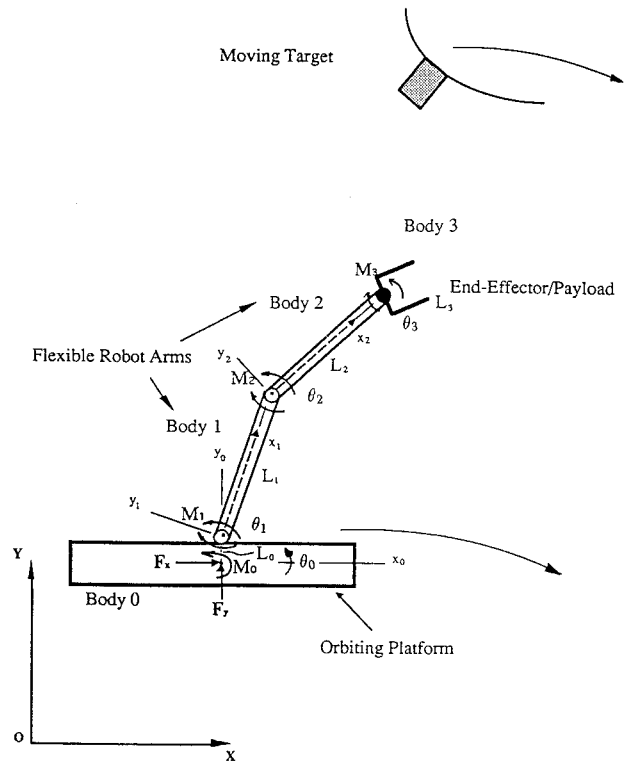

Fig. 1 Flexible space robot.

in which the system approaches an equilibrium point in the state space.

References 15 and 18 are concerned with flexible space robots of the type considered here, but the mission is more modest in scope. Indeed, in Ref. 15 the mission is to place a payload in a certain position and orientation in space and in Ref. 18 the objective is to dock with a target whose motion is known a priori.

In this paper, a control scheme permitting a flexible space robot to track and dock with a moving target whose motion is not known a priori is presented. For the robot maneuver, on-line feedback tracking control is carried out by means of an algorithm based on Lyapunov-like methodology and using on-line measurements of the target motion. For the vibration suppression, linear quadratic regulator (LQR) control in conjunction with disturbance compensation is carried out by means of collocated sensor/actuator pairs dispersed along the flexible arms. A modified discrete-time control scheme is developed, and problems related to the digital implementation of the control algorithms are discussed. The control algorithms are demonstrated by means of a numerical example.

II. Equations of Motion

We propose to derive the equations of motion by means of Lagrange's equations, which requires the kinetic energy, potential energy, and virtual work. To this end, we refer to Fig. 2, showing the flexible space robot and the coordinate systems used. Body 0 represents the robot base, assumed to be rigid. Bodies 1 and 2 are the robot manipulator arms attached in series to body 0, and they are flexible. Body 3 is the end effector/payload, also assumed to be rigid. For planar motion, the robot base is capable of two translations, x_0 and y_0, and one rotation, θ_0; the two flexible arms are capable of the rotations θ_1 and θ_2 and the elastic vibrations u_1 and u_2 and the end effector is capable of the rotation θ_3. Note that θ_0 is measured relative to the inertial axis X_1 and θ_i $(i = 1, 2, 3)$ are measured relative to the base axis x_0. Referring to Fig. 2, the displacement vector $\boldsymbol{U}_0$ and velocity vector $\boldsymbol{V}_0$ for a typical point in body 0 are as follows:

$$\boldsymbol{U}_0 = \boldsymbol{R} + C_0^T \boldsymbol{R}_0 \tag{2a}$$

$$\boldsymbol{V}_0 = \dot{\boldsymbol{R}} + C_0^T \tilde{\omega}_0 \boldsymbol{R}_0 \tag{2b}$$

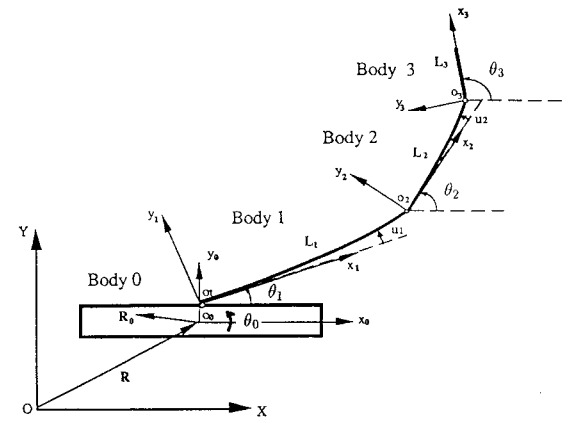

Fig. 2 Coordinate system for space robot.

Similarly, for body 1

$$\boldsymbol{U}_1 = \boldsymbol{R} + C_0^T \boldsymbol{L}_0 + C_1^T (\boldsymbol{r}_1 + \boldsymbol{u}_1) \tag{3a}$$

$$\boldsymbol{V}_1 = \dot{\boldsymbol{R}} + C_0^T \tilde{\omega}_0 \boldsymbol{L}_0 + C_1^T \tilde{\omega}_1 (\boldsymbol{r}_1 + \boldsymbol{u}_1) + C_1^T \dot{\boldsymbol{u}}_1 \tag{3b}$$

for body 2

$$\boldsymbol{U}_2 = \boldsymbol{R} + C_0^T \boldsymbol{L}_0 + C_1^T (\boldsymbol{L}_1 + \boldsymbol{u}_{12}) + C_2^T (\boldsymbol{r}_2 + \boldsymbol{u}_2) \tag{4a}$$

$$\boldsymbol{V}_2 = \dot{\boldsymbol{R}} + C_0^T \tilde{\omega}_0 \boldsymbol{L}_0 + C_1^T \tilde{\omega}_1 (\boldsymbol{L}_1 + \boldsymbol{u}_{12}) + C_1^T \dot{\boldsymbol{u}}_{12} + C_2^T \tilde{\omega}_2 (\boldsymbol{r}_2 + \boldsymbol{u}_2) + C_2^T \dot{\boldsymbol{u}}_2 \tag{4b}$$

and for body 3

$$\boldsymbol{U}_3 = \boldsymbol{R} + C_0^T \boldsymbol{L}_0 + C_1^T (\boldsymbol{L}_1 + \boldsymbol{u}_{12}) + C_2^T (\boldsymbol{L}_2 + \boldsymbol{u}_{23}) + C_3^T \boldsymbol{r}_3 \tag{5a}$$

$$\boldsymbol{V}_3 = \dot{\boldsymbol{R}} + C_0^T \tilde{\omega}_0 \boldsymbol{L}_0 + C_1^T \tilde{\omega}_1 (\boldsymbol{L}_1 + \boldsymbol{u}_{12}) + C_1^T \dot{\boldsymbol{u}}_{12} + C_2^T \tilde{\omega}_2 (\boldsymbol{L}_2 + \boldsymbol{u}_{23}) + C_2^T \dot{\boldsymbol{u}}_{23} + C_3^T \tilde{\omega}_e \boldsymbol{r}_3 \tag{5b}$$

where

$$C_i = \begin{bmatrix} \cos\theta_i & \sin\theta_i \\ -\sin\theta_i & \cos\theta_i \end{bmatrix}, \qquad i = 0, 1, 2, 3 \tag{6}$$

are matrices of direction cosines,

$$\tilde{\omega}_i = \begin{bmatrix} 0 & -\dot{\theta}_i \\ \dot{\theta}_i & 0 \end{bmatrix}, \qquad i = 0, 1, 2, 3 \tag{7}$$

are skew symmetric angular velocity matrices,

$$\boldsymbol{R} = [x_0 \quad y_0]^T, \qquad \boldsymbol{r}_1 = [x_1 \quad 0]^T, \qquad \boldsymbol{r}_2 = [x_2 \quad 0]^T \tag{8}$$

are position vectors, and

$$\boldsymbol{u}_1 = [0 \quad u_1]^T, \qquad \boldsymbol{u}_2 = [0 \quad u_2]^T \tag{9}$$

are elastic displacement vectors. Moreover,

$$u_{12} = u_1|_{x_1 = L_1}, \qquad u_{23} = u_2|_{x_2 = L_2} \tag{10}$$

The elastic displacements are discretized as follows:

$$u_i(x_i, t) = \boldsymbol{\Phi}_i^T(x_i)\boldsymbol{\xi}_i(t), \qquad i = 1, 2 \tag{11}$$

where $\boldsymbol{\Phi}_i(x_i)$ are vectors of quasicomparison functions[19] and $\boldsymbol{\xi}_i(t)$ are vectors of generalized displacements. Regarding the robot arms as beams in bending, the quasicomparison functions can be chosen as a linear combination of the admissible functions

$$\phi_k = \cosh\frac{\lambda_k x}{L} - \cos\frac{\lambda_k x}{L} - \sigma_k\left(\sinh\frac{\lambda_k x}{L} - \sin\frac{\lambda_k x}{L}\right) \qquad k = 1, 2, \ldots \tag{12}$$

which represent the eigenfunctions of a clamped-free beam for k odd and clamped-clamped beam for k even, where λ_k and σ_k are nondimensional parameters.

Using Eqs. (2–12), the kinetic energy of the system can be written as

$$T = \sum_{i=0}^{3} T_i = \frac{1}{2} \sum_{i=0}^{3} \int_{\text{body } i} \rho_i \boldsymbol{V}_i^T \boldsymbol{V}_i \, \mathrm{d}D_i = \frac{1}{2} \dot{\boldsymbol{q}}^T M \dot{\boldsymbol{q}} \tag{13}$$

where $\boldsymbol{q} = [\boldsymbol{R}^T \ \theta_0 \ \theta_1 \ \theta_2 \ \theta_3 \ \boldsymbol{\xi}_1^T \ \boldsymbol{\xi}_2^T]^T$ is the configuration vector and M is the mass matrix with entries given in Appendix A.

The potential energy for the system is due entirely to the elasticity of the robot arms and can be written in the form

$$V = \sum_{i=1}^{2} \frac{1}{2} \boldsymbol{\xi}_i^T K_i \boldsymbol{\xi}_i = \frac{1}{2} \boldsymbol{q}^T K \boldsymbol{q} \tag{14}$$

where

$$K = \text{block-diag}[0 \quad \bar{K}_1 \quad \bar{K}_2] \tag{15a}$$

$$\bar{K}_i = \int_0^{L_i} E I_i \boldsymbol{\Phi}_i''(\boldsymbol{\Phi}_i'')^T \mathrm{d}x_i, \qquad i = 1, 2 \tag{15b}$$

are the robot stiffness matrix and the stiffness matrices for bodies i, respectively, where in the latter EI_i denotes bending stiffnesses. Note that the gravitational potential is ignored here on the assumption that it represents a second-order effect.

The control forces acting on the robot system include the horizontal and vertical thrusts F_x and F_y acting at the base center, the external torque M_0 acting on the base, the internal joint torques M_1, M_2, and M_3 acting at the joints, and the distributed internal moments τ_1 and τ_2 generated by m_1 and m_2 actuators on links 1 and 2, respectively. We define the control force vector as $\boldsymbol{F} = [F_x \ F_y \ M_0 \ M_1 \ M_2 \ M_3 \ \tau_1^T \ \tau_2^T]^T$. Then, the virtual work of the system can be written in the form

$$\begin{aligned} \delta W = {} & F_x \, \delta x_0 + F_y \, \delta y_0 + M_0 \, \delta\theta_0 + M_1(\delta\theta_1 - \delta\theta_0) \\ & + M_2\big(\delta\theta_2 - \delta\theta_1 - \Phi_1'^T(L_1)\, \delta\boldsymbol{\xi}_1\big) \\ & + M_3\big(\delta\theta_3 - \delta\theta_2 - \Phi_2'^T(L_2)\, \delta\boldsymbol{\xi}_2\big) + \sum_{i=1}^{m_1} \tau_{1i} \Phi_1''^T(x_{1i})\, \delta\boldsymbol{\xi}_1 \\ & + \sum_{i=1}^{m_2} \tau_{2i} \Phi_2''^T(x_{2i})\, \delta\boldsymbol{\xi}_2 = \boldsymbol{Q}^T \delta\boldsymbol{q} \end{aligned} \tag{16}$$

where $\boldsymbol{Q}$ is a generalized force vector defined as

$$\boldsymbol{Q} = G\boldsymbol{F} \tag{17}$$

The entries of the matrix G are given in Appendix A.

Lagrange's equations for the system can be expressed in the symbolic vector form

$$\frac{\mathrm{d}}{\mathrm{d}t}\left(\frac{\partial T}{\partial \dot{\boldsymbol{q}}}\right) - \frac{\partial T}{\partial \boldsymbol{q}} + \frac{\partial V}{\partial \boldsymbol{q}} = \boldsymbol{Q} \tag{18}$$

Inserting Eqs. (13), (14), and (16) into Eq. (18), we obtain the system equations in the matrix form

$$M(\boldsymbol{q})\ddot{\boldsymbol{q}} + C(\boldsymbol{q}, \dot{\boldsymbol{q}})\dot{\boldsymbol{q}} + K\boldsymbol{q} = \boldsymbol{Q} \tag{19}$$

The entries of the matrix C are also given in Appendix A.

Equation (19) represents the equation governing the motion of the flexible space robot. It is used for computer simulation of the dynamic system. For the purpose of control design, Eq. (19) is conveniently separated into two sets of equations, rigid-body motion equations and elastic vibration equations. To this end, we write $\boldsymbol{q} = [\boldsymbol{q}_r^T \ \boldsymbol{q}_e^T]^T$ and $\boldsymbol{Q} = [\boldsymbol{Q}_r^T \ \boldsymbol{Q}_e^T]^T$, where $\boldsymbol{q}_r = [x_0 \ y_0 \ \theta_0 \ \theta_1 \ \theta_2 \ \theta_3]^T$ is a rigid-body displacement vector, $\boldsymbol{q}_e = [\boldsymbol{\xi}_1^T \ \boldsymbol{\xi}_2^T]^T$ is an elastic displacement vector, and $\boldsymbol{Q}_r$ and $\boldsymbol{Q}_e$ are corresponding generalized force vectors. Then Eq. (19) can be written in the partitioned matrix form

$$\begin{bmatrix} M_{rr} & M_{re} \\ M_{re}^T & M_{ee} \end{bmatrix} \begin{bmatrix} \ddot{\boldsymbol{q}}_r \\ \ddot{\boldsymbol{q}}_e \end{bmatrix} + \begin{bmatrix} C_{rr} & C_{re} \\ C_{er} & C_{ee} \end{bmatrix} \begin{bmatrix} \dot{\boldsymbol{q}}_r \\ \dot{\boldsymbol{q}}_e \end{bmatrix} + \begin{bmatrix} 0 & 0 \\ 0 & K \end{bmatrix} \begin{bmatrix} \boldsymbol{q}_r \\ \boldsymbol{q}_e \end{bmatrix} = \begin{bmatrix} \boldsymbol{Q}_r \\ \boldsymbol{Q}_e \end{bmatrix} \tag{20}$$

After some algebraic manipulations, and ignoring higher order terms in the elastic displacements, Eq. (20) can be separated into

$$M_r(\boldsymbol{q}_r)\ddot{\boldsymbol{q}}_r + C_r(\boldsymbol{q}_r, \dot{\boldsymbol{q}}_r)\dot{\boldsymbol{q}}_r + \boldsymbol{d}_e(\boldsymbol{q}, \dot{\boldsymbol{q}}, \ddot{\boldsymbol{q}}) = \boldsymbol{Q}_r \tag{21}$$

and

$$M_e(\boldsymbol{q}_r)\ddot{\boldsymbol{q}}_e + C_e(\boldsymbol{q}_r, \dot{\boldsymbol{q}}_r)\dot{\boldsymbol{q}}_e + K_e(\boldsymbol{q}_r, \dot{\boldsymbol{q}}_r, \ddot{\boldsymbol{q}}_r)\boldsymbol{q}_e + \boldsymbol{d}_r(\boldsymbol{q}_r, \dot{\boldsymbol{q}}_r, \ddot{\boldsymbol{q}}_r) = \boldsymbol{Q}_e \tag{22}$$

where M_r is the rigid-body part of the mass matrix M_{rr} and C_r is the rigid-body part of C_{rr}. Moreover, $M_e = M_{ee}$, $C_e = C_{ee}$, K_e consists of the stiffness matrix K and the part due to elasticity in the matrices M_{re} and C_{re}, and $\boldsymbol{d}_e$ and $\boldsymbol{d}_r$ are disturbance vectors. The entries of the various matrices are given in Appendix B. The term $\boldsymbol{d}_e$ in Eq. (21) is a linear combination of $\boldsymbol{q}_e$, $\dot{\boldsymbol{q}}_e$, and $\ddot{\boldsymbol{q}}_e$, with the matrices M_{re}, C_{re}, K_M^e, and K_C^e depending on $\boldsymbol{q}_r$, $\dot{\boldsymbol{q}}_r$, and $\ddot{\boldsymbol{q}}_r$, as shown in Eq. (B3) of Appendix B. It can be regarded as a disturbance due to the flexibility of the robot arms. The term $\boldsymbol{d}_r$ in Eq. (22) is a function of $\boldsymbol{q}_r$, $\dot{\boldsymbol{q}}_r$, and $\ddot{\boldsymbol{q}}_r$. It can be regarded as a disturbance due to the rigid-body maneuvering of the robot. Equations (21) and (22) are coupled. The coupling between rigid-body motions and flexible vibration is provided in Eq. (22) by the persistent disturbance $\boldsymbol{d}_r$ from the rigid-body motion, which causes the elastic motion $\boldsymbol{q}_e$, $\dot{\boldsymbol{q}}_e$, and $\ddot{\boldsymbol{q}}_e$. In turn, the elastic motion disturbs the rigid-body motion through $\boldsymbol{d}_e$ in Eq. (21). Equation (21) is used for the design of the maneuver control for tracking a moving target and Eq. (22) is used for design of control for vibration suppression.

III. Tracking Control Algorithm Using Lyapunov-like Methodology

In this section, the general idea of Lyapunov-like methodology for tracking control developed for rigid robots[9] is introduced.

The dynamic equation of a rigid robot is given by

$$M(\boldsymbol{q})\ddot{\boldsymbol{q}} + C(\boldsymbol{q}, \dot{\boldsymbol{q}})\dot{\boldsymbol{q}} = \boldsymbol{Q} \tag{23}$$

and the kinematic relation between the robot configuration vector $\boldsymbol{q}$ and robot output vector $\boldsymbol{y}_e$ is given by

$$\boldsymbol{y}_e = \boldsymbol{f}(\boldsymbol{q}) \tag{24}$$

so that

$$\dot{\boldsymbol{y}}_e = J(\boldsymbol{q})\dot{\boldsymbol{q}} \tag{25a}$$

$$\ddot{\boldsymbol{y}}_e = J(\boldsymbol{q})\ddot{\boldsymbol{q}} + \dot{J}(\boldsymbol{q}, \dot{\boldsymbol{q}})\dot{\boldsymbol{q}} \tag{25b}$$

where $J(\boldsymbol{q}) = [\partial \boldsymbol{f}/\partial \boldsymbol{q}]$ is the Jacobian matrix.

Because tracking is carried out by the end effector, the tracking problem consists of driving the error $\boldsymbol{e} = \boldsymbol{y}_t - \boldsymbol{y}_e$ and its time derivative $\dot{\boldsymbol{e}}$ to zero. To this end, a Lyapunov function is defined by

$$V = \tfrac{1}{2} \boldsymbol{z}^T \boldsymbol{z} \tag{26a}$$

where

$$\boldsymbol{z} = (\dot{\boldsymbol{e}} + \beta \boldsymbol{e}) \tag{26b}$$

in which β is a positive scalar. If the control is designed in such a way that

$$\dot{V} = -\sigma V \tag{27a}$$

$$\sigma = \frac{\ell n(V_0/\epsilon)}{t_s} \tag{27b}$$

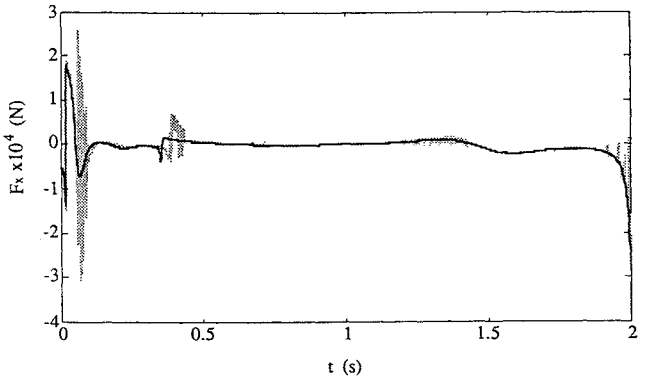

Fig. 3 Bursting phenomenon.

where ϵ is an arbitrarily small positive scalar and V_0 is the initial value of V, it is guaranteed that the function V remains in the ϵ neighborhood of zero for $t > t_s$, no matter how the target motion changes. This ensures that the error $\boldsymbol{e}$ and its derivative $\dot{\boldsymbol{e}}$ are also very close to zero.

We consider the nonlinear control law

$$\boldsymbol{Q} = M(\boldsymbol{q})\boldsymbol{u}_r + C(\boldsymbol{q}, \dot{\boldsymbol{q}})\dot{\boldsymbol{q}} \tag{28}$$

where $\boldsymbol{u}_r$ is chosen in the form[9]

$$\boldsymbol{u}_r = [(h_1 + h_2)/\Delta]\boldsymbol{w} \tag{29a}$$

$$\Delta = \begin{cases} z^T J\boldsymbol{w} & \text{if} \quad z^T J\boldsymbol{w} \geq \delta \\ \delta & \text{if} \quad z^T J\boldsymbol{w} < \delta \end{cases} \tag{29b}$$

in which δ is a small positive scalar, $\boldsymbol{w}$ is an arbitrarily chosen vector, and

$$h_1 = z^T(\ddot{\boldsymbol{y}}_t - \dot{J}\dot{\boldsymbol{q}} + \beta\dot{\boldsymbol{e}}) \tag{30a}$$

$$h_2 = 0.5\sigma z^T z = \sigma V \tag{30b}$$

It can be shown that the control algorithm described above yields the desired result, i.e., Eqs. (27a) and (27b).

The control algorithm possesses the following advantages:

1) The control decision is made using on-line information of the current robot state $(\boldsymbol{q}, \dot{\boldsymbol{q}})$ and target state $(\boldsymbol{e}, \dot{\boldsymbol{e}}, \text{ and } \ddot{\boldsymbol{y}}_t)$. The feedback control can automatically counteract adverse disturbances in space and achieve the final docking in an accurate and smooth way.

2) The on-line calculation is relatively simple, as it involves neither inverse kinematics nor matrix inversions.

3) Stability is always guaranteed by Lyapunov stability theorem, as can be seen from Eqs. (27), no matter how the target motion changes.

However, after applying the above algorithm directly to our space robot system and simulating the system in both continuous time and discrete time, the results from a discrete-time system exhibited some undesirable phenomenon, although the performance of the continuous system was good. As shown in Fig. 3, in which the solid line denotes continuous-time results and the dashed line denotes discrete-time results, the control force in discrete time exhibits periods of oscillatory behavior. Further numerical simulations show that the magnitude of the control force during chattering is bounded, although very large, and its mean value is close to the results of the corresponding continuous-time system. Moreover, the occurrence of the oscillating period is random, and the length of the oscillating periods and the length of the "good performance" periods are both unpredictable. This phenomenon is similar to the so-called bursting, which appears frequently in discrete-time adaptive systems and has been reported for almost a decade.[20] Due to the complexity of our space robot, it is difficult to identify clearly the source of the bursting phenomenon. However, because the phenomenon is not reported in Ref. 9, in which a nonredundant robot is simulated in discrete time, we can conjecture that in the case at hand, the phenomenon is related to robot redundancy. It is important to keep the control force from bursting. Otherwise the possibility exists that the control cannot be realized. To this end, a modified version of the above algorithm is presented, which also takes into account the flexibility of the robot arms.

IV. Modified Tracking Control Algorithm for Flexible Space Robots

To apply Lyapunov-like methodology to flexible space robots, we first extend the kinematical relation given by Eq. (26) to flexible space robots as follows:

$$\begin{aligned} x_e &= x_0 - L_0\sin\theta_0 + L_1\cos\theta_1 + L_2\cos\theta_2 \\ &\quad + L_3\cos\theta_3 - u_{12}\sin\theta_1 - u_{23}\sin\theta_2 \\ y_e &= y_0 + L_0\cos\theta_0 + L_1\sin\theta_1 + L_2\sin\theta_2 + L_3\sin\theta_3 \\ &\quad + u_{12}\cos\theta_1 + u_{23}\cos\theta_2 \\ \theta_e &= \theta_3 \end{aligned} \tag{31}$$

For kinematical analysis, we define $\bar{\boldsymbol{q}} = [\boldsymbol{q}_r^T \ \ \boldsymbol{q}_u^T]^T$, where $\boldsymbol{q}_r$ was defined earlier and $\boldsymbol{q}_u = [u_{12} \ \ u_{23}]^T$. The Jacobian matrix $\bar{J}$, obtained by differentiating Eq. (31) with respect to $\bar{\boldsymbol{q}}$, has the form $\bar{J} = [J_r \ \ J_u]$, where

$$J_r = \begin{bmatrix} 1 & 0 & -L_0\cos\theta_0 & -L_1\sin\theta_1 - u_{12}\cos\theta_1 & -L_2\sin\theta_2 - u_{23}\cos\theta_2 & -L_3\sin\theta_3 \\ 0 & 1 & -L_0\sin\theta_0 & L_1\cos\theta_1 - u_{12}\sin\theta_1 & L_2\cos\theta_2 - u_{23}\sin\theta_2 & L_3\cos\theta_3 \\ 0 & 0 & 0 & 0 & 0 & 1 \end{bmatrix} \tag{32a}$$

$$J_u = \begin{bmatrix} -\sin\theta_1 & -\sin\theta_2 \\ \cos\theta_1 & \cos\theta_2 \\ 0 & 0 \end{bmatrix} \tag{32b}$$

Hence, we can write the relations

$$\dot{\boldsymbol{y}}_e = \bar{J}\dot{\bar{\boldsymbol{q}}} \tag{33a}$$

$$\ddot{\boldsymbol{y}}_e = \bar{J}\ddot{\bar{\boldsymbol{q}}} + \dot{\bar{J}}\dot{\bar{\boldsymbol{q}}} \tag{33b}$$

The dynamical equation for the rigid-body motion of the space robot is given by Eq. (21). We first define a nonlinear control law for $\boldsymbol{Q}_r$ as follows:

$$\boldsymbol{Q}_r = M_r(\boldsymbol{q}_r)\boldsymbol{u}_r + C_r(\boldsymbol{q}_r, \dot{\boldsymbol{q}}_r)\dot{\boldsymbol{q}}_r \tag{34}$$

Substituting Eq. (34) into Eq. (21), we obtain

$$\ddot{\boldsymbol{q}}_r = \boldsymbol{u}_r - M_r^{-1}\boldsymbol{d}_e \tag{35}$$

To prevent the bursting phenomenon, we propose decoupled Lyapunov functions

$$V_i = \tfrac{1}{2}z_i^2, \qquad i = 1, 2, 3 \tag{36a}$$

$$z_i = \dot{e}_i + \beta e_i, \qquad i = 1, 2, 3 \tag{36b}$$

Taking the derivative of Eq. (36a) and using Eqs. (33) and (35), we obtain

$$\dot{V}_i = z_i h_i - z_i\left([J_r\boldsymbol{u}_r]_i - \left[J_r M_r^{-1}\boldsymbol{d}_e\right]_i\right), \qquad i = 1, 2, 3 \tag{37}$$

where $[\cdot]_i$ denotes the ith element of a vector and h_i are the components of the vector

$$\boldsymbol{h} = \ddot{\boldsymbol{y}}_t - \dot{\tilde{J}}\dot{\boldsymbol{q}} + \beta\dot{\boldsymbol{e}} - J_u\ddot{\boldsymbol{q}}_u \tag{38}$$

Because M_r is a positive definite matrix, M_r^{-1} is bounded, and we note that J_r is also bounded. Moreover, from Eq. (B3) in Appendix B, we see that $\boldsymbol{d}_e$ is a linear combination of $\boldsymbol{q}_e$, $\dot{\boldsymbol{q}}_e$, and $\ddot{\boldsymbol{q}}_e$. We then assume that $\boldsymbol{d}_e$ is bounded in accordance with our ultimate goal of vibration suppression. Hence, we can assume that the term $[J_r M_r^{-1}\boldsymbol{d}_e]_i$ is bounded and satisfies the relation

$$\left[J_r M_r^{-1}\boldsymbol{d}_e\right]_i < \delta_i, \qquad i = 1, 2, 3 \tag{39}$$

From Eq. (39), we have

$$z_i\left[J_r M_r^{-1}\boldsymbol{d}_e\right]_i < |z_i|\delta_i, \qquad i = 1, 2, 3 \tag{40}$$

If we can determine a vector $\boldsymbol{u}_r$ that satisfies the conditions

$$z_i[J_r\boldsymbol{u}_r]_i = z_i h_i + \tfrac{1}{2}\alpha_i z_i^2 + |z_i|\delta_i, \qquad i = 1, 2, 3 \tag{41}$$

then

$$\dot{V}_i = -\tfrac{1}{2}\alpha_i z_i^2 + z_i\left[J_r M_r^{-1}\boldsymbol{d}_e\right]_i - |z_i|\delta_i < -\tfrac{1}{2}\alpha_i z_i^2 = -\alpha_i V_i, \qquad i = 1, 2, 3 \tag{42}$$

According to the Lyapunov stability theorem, Eq. (41) is the sufficient condition for our tracking problem. We further simplify Eq. (41) by assuming $z_i \neq 0$, so that

$$[J_r\boldsymbol{u}_r]_i = h_i + \tfrac{1}{2}\alpha_i z_i + \operatorname{sgn}(z_i)\delta_i, \qquad i = 1, 2, 3 \tag{43}$$

or

$$[J_r\boldsymbol{u}_r]_i = s_i, \qquad i = 1, 2, 3 \tag{44}$$

with

$$s_i = \ddot{y}_{ti} - [\dot{\tilde{J}}\dot{\boldsymbol{q}}]_i + \beta\dot{e}_i - [J_u\ddot{\boldsymbol{q}}_u]_i + \tfrac{1}{2}\alpha_i z_i + \operatorname{sgn}(z_i)\delta_i \tag{45}$$

Equation (44) can be expressed in the matrix form

$$J_r\boldsymbol{u}_r = \boldsymbol{s} \tag{46}$$

where $\boldsymbol{s} = [s_1\ s_2\ s_3]^T$ and J_r is a 3×6 matrix. The solution of Eq. (46) does not yield a unique $\boldsymbol{u}_r$. This agrees with Eq. (29) in the original control scheme in which $\boldsymbol{w}$ is an arbitrarily chosen vector. Here we can simply prescribe the redundant degrees of freedom and then solve Eq. (46) accordingly.

As a simple example, we constrain three components of $\boldsymbol{u}_r$ by taking

$$u_{r3} = u_{r4} = u_{r5} = 0 \tag{47}$$

for the entire tracking period and use Eq. (46) to solve for the other three components of $\boldsymbol{u}_r$ on-line, with the result

$$u_{r1} = s_1 + L_3 \sin\theta_3 u_{r6}, \qquad u_{r2} = s_2 - L_3\cos\theta_3 u_{r6},$$
$$u_{r6} = s_3 \tag{48}$$

The above algorithm for $\boldsymbol{u}_r$, together with Eq. (34), represents the maneuver control for a flexible space robot tracking a moving target whose motion is not known a priori. The control algorithm requires that the following conditions be satisfied:

1) The output error vector $\boldsymbol{e}$ and its time derivative $\dot{\boldsymbol{e}}$ can be measured on-line.

2) The target output acceleration $\ddot{\boldsymbol{y}}_t$ can be measured or estimated on-line.

3) The robot rigid-body displacement vector $\boldsymbol{q}_r$ and its time derivative $\dot{\boldsymbol{q}}_r$ can be measured on-line.

4) The elastic tip displacement vector $\boldsymbol{q}_u$ and its time derivatives $\dot{\boldsymbol{q}}_u$ and $\ddot{\boldsymbol{q}}_u$ can be measured on-line.

5) The elastic vibration of the robot arms should be controlled so that a reasonable value for the upper bound δ_i can be set.

In addition to the advantages of the original algorithm mentioned in Sec. III, the modified control algorithm presented here provides two extensions from the original one.[9] The first extension is that the flexible effect of the robot arms is incorporated into the control algorithm. It is reflected in the kinematic relations expressed by Eqs. (31) and in the term $\operatorname{sgn}(z_i)\delta_i$ in Eq. (45), which is associated with the vibration disturbance vector $\boldsymbol{d}_e$ in Eq. (21). The second extension consists of the use of decoupled Lyapunov functions [Eqs. (36)] to eliminate the bursting phenomenon (Sec. III) when the control algorithm is implemented in discrete time.

V. Vibration Control

Because of coupling between the rigid-body motions and the elastic vibration, the performance of the tracking control depends on how well the vibration suppression is carried out. Without vibration control, the tracking cannot be truly realized for a flexible space robot. Our objective is to drive the elastic motion state $\boldsymbol{q}_e$, $\dot{\boldsymbol{q}}_e$ close to zero during the tracking and docking operation. We recall that the motion of the elastic vibration of the space robot is described by Eq. (22), which represents a linear time-varying system with a persistent disturbance term $\boldsymbol{d}_r$ due to the rigid-body motions.

We propose to control the vibration in discrete time. To this end, we separate the generalized control force $\boldsymbol{Q}_e$ into

$$\boldsymbol{Q}_e(k) = \boldsymbol{Q}_{er}(k) + \boldsymbol{Q}_{ee}(k) \tag{49}$$

The discrete-time control algorithm for disturbance compensation is expressed by

$$\boldsymbol{Q}_{er}(k) = \boldsymbol{d}_r(\boldsymbol{q}_r(k), \dot{\boldsymbol{q}}_r(k), \ddot{\boldsymbol{q}}_r(k)) \tag{50}$$

If the disturbance is canceled perfectly, Eq. (24) becomes

$$M_e(\boldsymbol{q}_r)\ddot{\boldsymbol{q}}_e + C_e(\boldsymbol{q}_r, \dot{\boldsymbol{q}}_r)\dot{\boldsymbol{q}}_e + K_e(\boldsymbol{q}_r, \dot{\boldsymbol{q}}_r, \ddot{\boldsymbol{q}}_r)\boldsymbol{q}_e = \boldsymbol{Q}_{ee} \tag{51}$$

Letting $\boldsymbol{x}(k) = [\boldsymbol{q}_e(k)^T\ \ \dot{\boldsymbol{q}}_e(k)^T]^T$ be the state vector and $\boldsymbol{u}(k) = \boldsymbol{Q}_{ee}(k)$ the control vector, the discrete-time state space counterpart of Eq. (51) can be written as

$$\boldsymbol{x}(k+1) = \hat{A}(k)\boldsymbol{x}(k) + \hat{B}(k)\boldsymbol{u}(k) \tag{52}$$

where the coefficient matrices are given by

$$\hat{A}(k) = e^{A(kT)} \tag{53a}$$

$$\hat{B}(k) = (e^{A(kT)} - I)A^T(kT)B(kT) \tag{53b}$$

in which

$$A(t) = \begin{bmatrix} 0 & I \\ -M_e^{-1}K_e & -M_e^{-1}C_e \end{bmatrix} \tag{54a}$$

$$B(t) = \begin{bmatrix} 0 \\ M_e^{-1} \end{bmatrix} \tag{54b}$$

The performance index for the discrete-time LQR is given by[21]

$$\hat{J} = \frac{1}{2}\sum_{k=0}^{N}[\boldsymbol{x}^T(k)Q(k)\boldsymbol{x}(k) + \boldsymbol{u}^T(k)R\boldsymbol{u}(k)] \tag{55}$$

yielding the control law

$$\boldsymbol{u}(k) = -[R + \hat{B}(k)\hat{K}(k)\hat{B}(k)]^{-1}\hat{B}^T(k)\hat{K}(k)\hat{A}(k)\boldsymbol{x}(k) \tag{56}$$

where $\hat{K}(k)$ satisfies the discrete-time algebraic Riccati equation

$$\hat{K}(k) = \hat{A}^T(k)[\hat{K}(k) - \hat{K}(k)\hat{B}(k)[R + \hat{B}^T(k)\hat{K}(k)\hat{B}(k)]^{-1} \times \hat{B}^T(k)\hat{K}(k)]\hat{A}(k) + Q \tag{57}$$

Direct application of the discrete-time control algorithm described by Eqs. (50) and (56) to our problem causes severe instability. The reason is that the discrete-time control force $\boldsymbol{Q}_{er}$ in Eq. (50) is not

able to cancel the continuous disturbance term $\boldsymbol{d}_r$ in Eq. (22) perfectly. Hence, the LQR control design based on Eq. (51), in which the disturbance is absent, is no longer appropriate. The error accumulates with time and it finally results in instability. To resolve this problem, a modified vibration control algorithm is proposed in the next section.

VI. Modified Discrete-Time Vibration Control Algorithm

An examination of the disturbance term $\boldsymbol{d}_r$ in Eq. (B14) of Appendix B, i.e., an examination of

$$\boldsymbol{d}_r = M_{re}^T \ddot{\boldsymbol{q}}_r + C_{er}\dot{\boldsymbol{q}}_r \tag{58}$$

reveals that $\ddot{\boldsymbol{q}}_r$ in the first term is the major cause of the system instability. Usually $\ddot{\boldsymbol{q}}_r(k)$ is not available and $\ddot{\boldsymbol{q}}_r(k-1)$ is used as an estimate of $\ddot{\boldsymbol{q}}_r(k)$. Stable performance of the system can be achieved only if $\ddot{\boldsymbol{q}}_r(k)$ can be measured or estimated perfectly. Even a very small error in $\ddot{\boldsymbol{q}}_r$ appearing in Eq. (58) can result in failure of the LQR design. To avoid use of $\ddot{\boldsymbol{q}}_r$ in Eq. (58), we replace $\dot{\boldsymbol{q}}_r$ by $\boldsymbol{u}_r$, so that the disturbance compensation scheme becomes

$$\begin{aligned}\boldsymbol{Q}_{er}(k) &= \boldsymbol{d}_r(\boldsymbol{q}_r(k), \dot{\boldsymbol{q}}_r(k), \boldsymbol{u}_r(k)) \\ &= M_{re}^T(\boldsymbol{q}_r(k))\boldsymbol{u}_r(k) + C_{er}(\boldsymbol{q}_r(k), \dot{\boldsymbol{q}}_r(k))\dot{\boldsymbol{q}}_r(k)\end{aligned} \tag{59}$$

where $\boldsymbol{u}_r(k)$ is calculated by the tracking control algorithm given by Eq. (46). We then substitute Eqs. (58), (59), and (35) into Eq. (22) and obtain the system equation as follows:

$$M_e(\boldsymbol{q}_r)\ddot{\boldsymbol{q}}_e + C_e(\boldsymbol{q}_r, \dot{\boldsymbol{q}}_r)\dot{\boldsymbol{q}}_e + K_e(\boldsymbol{q}_r, \dot{\boldsymbol{q}}_r, \ddot{\boldsymbol{q}}_r)\boldsymbol{q}_e - M_{re}^T M_r^{-1}\boldsymbol{d}_e = \boldsymbol{Q}_{ee} \tag{60}$$

As shown in Appendix B, $\boldsymbol{d}_e$ can be expressed as

$$\boldsymbol{d}_e = M_{re}\ddot{\boldsymbol{q}}_e + C_{re}\dot{\boldsymbol{q}}_e + \left(K_M^e + K_C^e\right)\boldsymbol{q}_e \tag{61}$$

where K_M^e and K_C^e are given by Eqs. (B6) and (B8), respectively. Substituting Eq. (61) into Eq. (60), we obtain the modified linear time-varying system

$$M_e^*(\boldsymbol{q}_r)\ddot{\boldsymbol{q}}_e + C_e^*(\boldsymbol{q}_r, \dot{\boldsymbol{q}}_r)\dot{\boldsymbol{q}}_e + K_e^*(\boldsymbol{q}_r, \dot{\boldsymbol{q}}_r, \ddot{\boldsymbol{q}}_r)\boldsymbol{q}_e = \boldsymbol{Q}_{ee} \tag{62}$$

where, comparing Eqs. (56) and (67), we observe that matrices M_e^*, C_e^*, and K_e^* represent modified coefficient matrices given by

$$M_e^* = M_e - M_{re}^T M_r^{-1} M_{re} \tag{63a}$$

$$C_e^* = C_e - M_{re}^T M_r^{-1} C_{re} \tag{63b}$$

$$K_e^* = K_e - M_{re}^T M_r^{-1}\left(K_M^e + K_C^e\right) \tag{63c}$$

Based on Eqs. (62) and (63), we can follow the same procedure as in Sec. V and obtain the control law for $\boldsymbol{Q}_{ee}$. The simulation results using the modified control scheme showed stable performance. Further numerical simulations showed that, even in the case of a system with only the mass matrix M_e modified, i.e., a system described by

$$M_e^*(\boldsymbol{q}_r)\ddot{\boldsymbol{q}}_e + C_e(\boldsymbol{q}_r, \dot{\boldsymbol{q}}_r)\dot{\boldsymbol{q}}_e + K_e(\boldsymbol{q}_r, \dot{\boldsymbol{q}}_r, \ddot{\boldsymbol{q}}_r)\boldsymbol{q}_e = \boldsymbol{Q}_{ee} \tag{64}$$

the LQR control law is still able to produce good system performance. This is because the first term on the right side of Eq. (61) is dominant, so that using C_e and K_e instead of C_e^* and K_e^*, respectively, is equivalent to dropping the second and third terms in Eq. (61), which does not affect the system performance very much. Note that the control gains are time varying, so that they must be updated repeatedly.

VII. Numerical Example

We assume that the parameters for the flexible space robot shown in Fig. 1 have the values

$$\begin{aligned} &m_0 = 40.0\text{ kg}, \quad m_1 = m_2 = 10.0\text{ kg}, \quad m_3 = 2.0\text{ kg} \\ &L_0 = 2.5\text{ m}, \quad L_1 = L_2 = 10.0\text{ m}, \quad L_3 = 2.0\text{ m} \\ &S_x = S_y = 0, \quad I_x = 83.333\text{ kg m}^2 \\ &I_y = 333.333\text{ kg m}^2, \quad EI_1 = EI_2 = 10^4\text{ kg m}^2 \end{aligned} \tag{65}$$

The target motion is not known a priori and must be measured on-line. However, for simulation purposes, we choose an example target trajectory as follows:

$$\begin{aligned} &x_t(t) = 10.0\sin\left(\frac{\pi}{10}t\right), \quad y_t(t) = 10.0 + 10.0\sin\left(\frac{\pi}{10}t\right) \\ &\theta_t(t) = \frac{3\pi}{20}t, \quad t \in [0, 5.0\text{ s}] \end{aligned} \tag{66}$$

The initial conditions of the space robot are given by

$$\begin{aligned} &\boldsymbol{q}_r(0) = [0.0 \quad -15.0 \quad 0.0 \quad 0.5\pi \quad 0.4775\pi \quad 0.25\pi]^T \\ &\dot{\boldsymbol{q}}_r(0) = \boldsymbol{0} \\ &\boldsymbol{q}_e(0) = [0.01 \cdots 0.01]^T, \quad \dot{\boldsymbol{q}}_e(0) = \boldsymbol{0} \end{aligned} \tag{67}$$

The parameters of the control synthesis design are

$$\beta = 20.0, \quad \epsilon = 10^{-3}, \quad t_s = 2.5\text{ s}, \quad \delta_i = 20 \quad i = 1, 2, 3 \tag{68}$$

We designate the three redundant degrees of freedom in $\boldsymbol{u}_r$ as u_{r3}, u_{r4}, and u_{r5}. They are defined for two different cases as follows:

Case 1:

$$u_{r3} = u_{r4} = u_{r5} = 0, \quad 0 \le t \le 5\text{ s} \tag{69}$$

Case 2:

$$u_{r3} = \begin{cases} 0, & t \le 0 \\ 4\,\Delta\theta_0/t_f^2, & 0 < t \le t_f/2 \\ -4\,\Delta\theta_0/t_f^2, & t_f/2 < t \le t_f \\ 0, & t > t_f \end{cases} \tag{70a}$$

$$u_{r4} = \begin{cases} 0, & t \le 0 \\ 4\,\Delta\theta_1/t_f^2, & 0 < t \le t_f/2 \\ -4\,\Delta\theta_1/t_f^2, & t_f/2 < t \le t_f \\ 0, & t > t_f \end{cases} \tag{70b}$$

$$u_{r5} = \begin{cases} 0, & t \le 0 \\ 4\,\Delta\theta_2/t_f^2, & 0 < t \le t_f/2 \\ -4\,\Delta\theta_2/t_f^2, & t_f/2 < t \le t_f \\ 0, & t > t_f \end{cases} \tag{70c}$$

where $t_f = 4.0$ s, $\Delta\theta_0 = \pi/6$ rad, $\Delta\theta_1 = \pi/4$ rad, and $\Delta\theta_2 = -\pi/6$ rad.

For a rigid space robot, Eqs. (69) and (70) represent constraints on the acceleration of the robot configuration. In case 1, the mission amounts to keeping the base attitude θ_0 and the two joint angles θ_1 and θ_2 constant while tracking a moving target. In case 2, the mission implies bang-bang maneuvers involving a base attitude change of $\Delta\theta_0$ and arms angle changes of $\Delta\theta_1$ and $\Delta\theta_2$ while tracking a moving target.

The constraints cannot be realized perfectly for a flexible space robot due to disturbance-causing vibration. However, the performance can be improved by vibration control. Because the major objective here is to track the moving target, we use the constraint equations (69) and (70) to eliminate the robot redundancy.

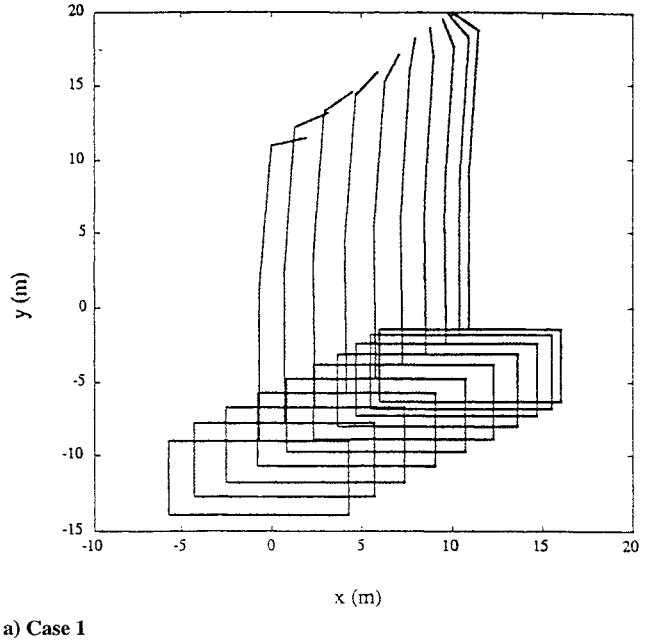

a) Case 1

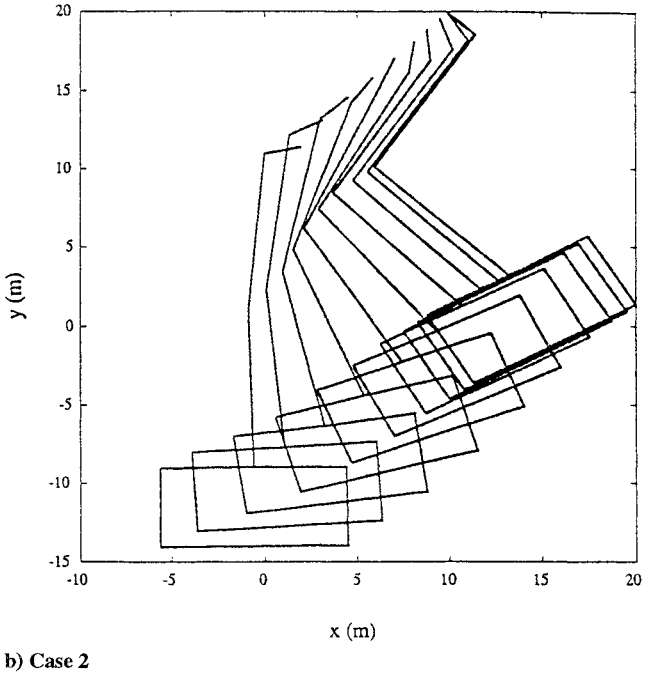

b) Case 2

Fig. 4 Time-lapse picture of robot configuration.

Note that to prevent chattering in simulations sgn(z) in Eq. (45) was replaced by

$$\text{sat}(z) = \begin{cases} \text{sgn}(z) & \text{for} \quad |z| \geq \epsilon \\ z & \text{for} \quad z < \epsilon \end{cases} \tag{71}$$

where ϵ is a small positive number.

For vibration control, the LQR design parameters are chosen as

$$R = \text{diag}[I_{n\times n} \;\; I_{n\times n}]$$

$$Q = \text{diag}\left[2.0 \times 10^4 I_{n\times n} \;\; 10^4 I_{n\times n} \;\; 2.0 \times 10^4 I_{n\times n} \;\; 10^4 I_{n\times n}\right] \tag{72}$$

The elastic displacement for each of the two arms was modeled by means of five quasicomparison functions.[19]

The elastic deformations are controlled by means of five collocated actuator/sensor pairs, so that $m_i = 5$ and $x_{ij} = (j/5)L_i$ $(i = 1, 2, j = 1, 2, \ldots, 5)$. The control forces generated by these actuators are transformed into generalized control forces by means of Eq. (17), with the matrix G being given by Eqs. (A7) and (A8). Of course, the sensor measurements $u_i(x_{ij}, t)$ $(i = 1, 2, \; j = 1, 2, \ldots, 5)$ are related to the generalized elastic displacement vectors $\boldsymbol{\xi}_i(t)$ $(i = 1, 2)$ through Eq. (11).

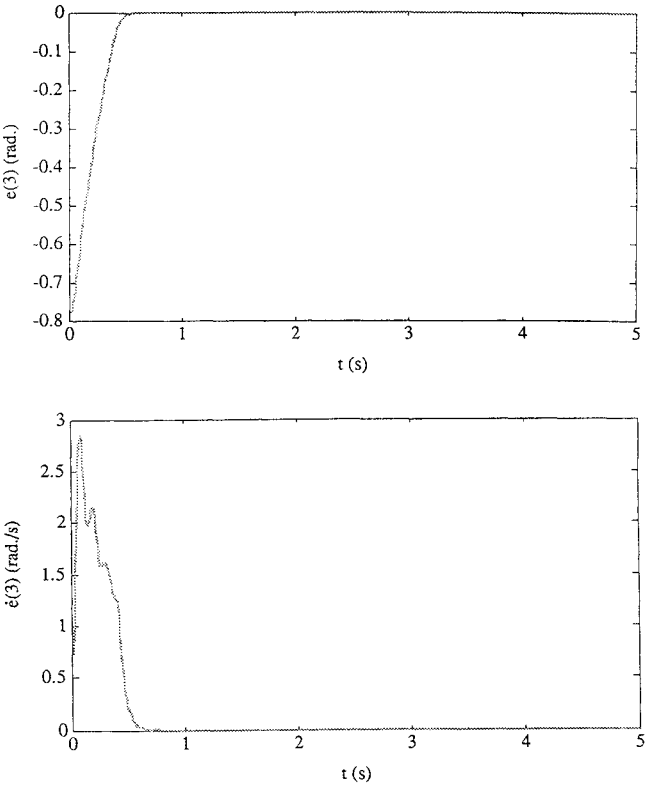

Fig. 5 Time history of orientation error and orientation error rate: case 2.

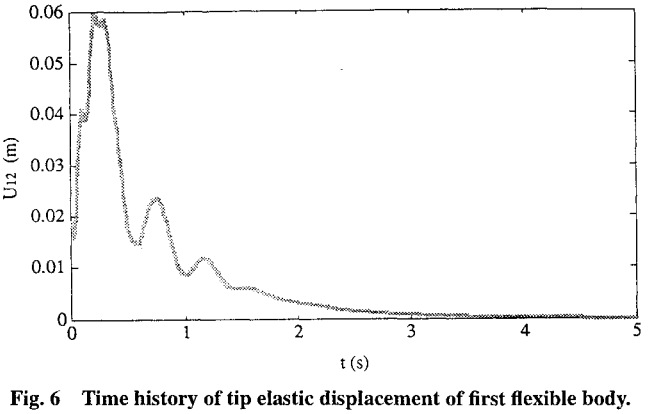

Fig. 6 Time history of tip elastic displacement of first flexible body.

The system performance under the tracking and docking maneuver is simulated over 5 s. To this end, the tracking control algorithm presented in Sec. IV and the vibration control algorithm presented in Sec. VI are used. The simulation is performed in discrete time with a sampling period $T = 0.001$ s.

Figures 4a and 4b show time-lapse pictures of the robot configuration for cases 1 and 2, respectively. For case 2, time histories of the orientation tracking error $e(3)$ and its time derivative $\dot{e}(3)$ are shown in Fig. 5, the time history of the tip elastic displacement of the first flexible link is shown in Fig. 6, and time histories of the control force F_x and torques M_0 and M_3 for the rigid-body maneuver are displayed in Figs. 7a–7c. Time histories of the control torque $\tau_2(3)$ acting on the second flexible body for disturbance rejection and LQR control are shown in Figs. 8 and 9, respectively. The results are very satisfactory, with control achieved in less than 1 s.

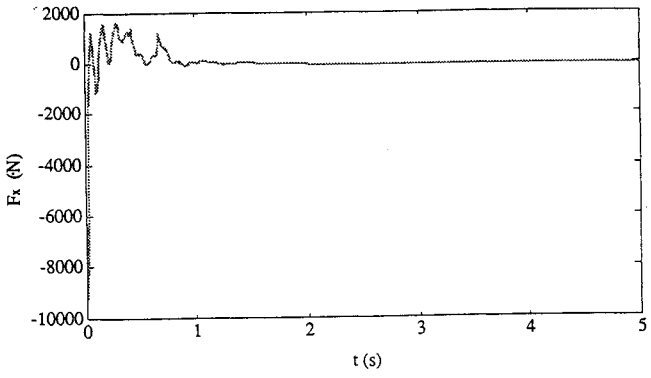

Fig. 7a Time history of control force for translation of base in x direction.

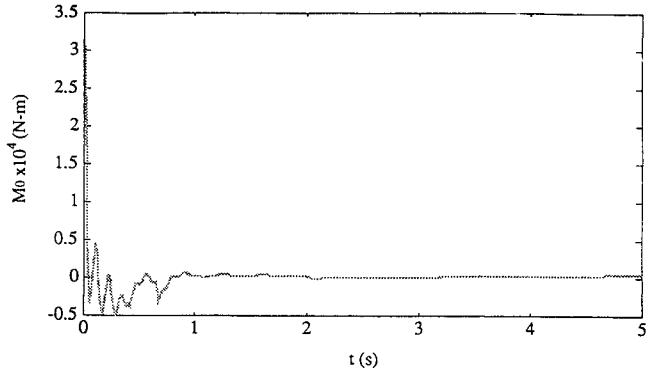

Fig. 7b Time history of control torque for rotation of base.

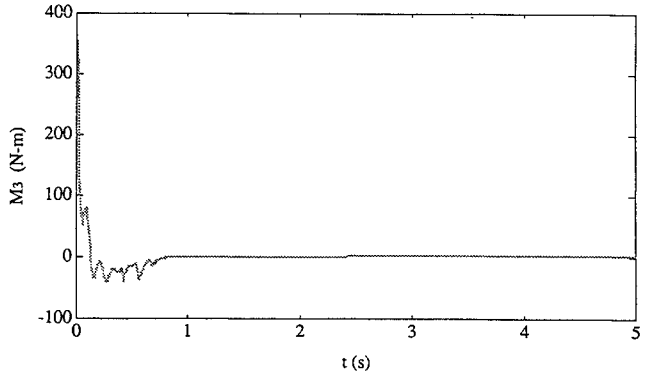

Fig. 7c Time history of control torque for rotation of body 3.

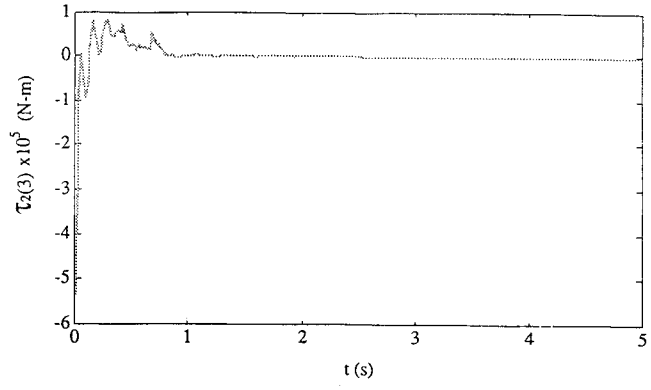

Fig. 8 Time history of control torque acting on body 2 for disturbance rejection.

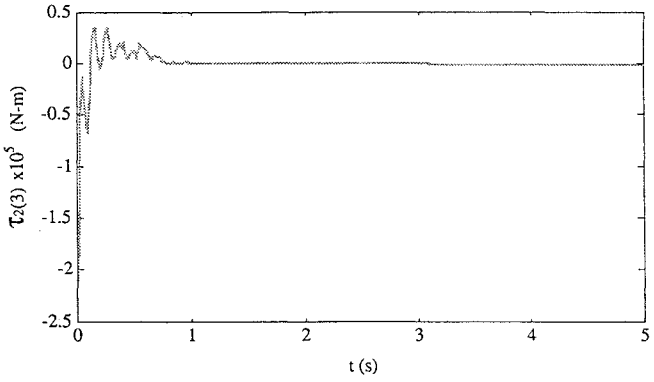

Fig. 9 Time history of LQR control torque acting on body 2.

VIII. Summary and Conclusions

This paper is concerned with the control of a flexible space robot executing a docking maneuver with a target whose motion is not known a priori. The control is based on on-line measurements of the target motion. The dynamical equations of the space robot are first derived by means of Lagrange's equations and then separated into two coupled sets of equations suitable for rigid-body maneuvers and vibration suppression. Controls for the rigid-body maneuver and vibration suppression are developed and implemented in discrete time. Problems arising from digital implementation of the control algorithms are discussed. Then, modifications of the control algorithms so as to prevent the problems are made.

The control scheme presented can be applied to two-dimensional as well as three-dimensional problems. Furthermore, it has the flexibility of solving different problems by defining appropriate output vectors other than the end-effector output vector. For example, if the mission involves tracking and docking with an orbiting target while its base attitude is to be kept constant, we can define the output vector as $\boldsymbol{y}_e = [x_e \;\; y_e \;\; \theta_e \;\; \theta_0]^T$ and the target output vector as $\boldsymbol{y}_t = [x_t \;\; y_t \;\; \theta_t \;\; 0]^T$, and then the proposed tracking control algorithm can be used to drive the error vector $\boldsymbol{e} = \boldsymbol{y}_t - \boldsymbol{y}_e$ and its time derivative $\dot{\boldsymbol{e}}$ to zero.

A numerical example is used to demonstrate the control scheme. The simulation results have shown very good system performance in both the tracking maneuver and the vibration suppression.

Appendix A: Matrices in Equations of Motion

The mass matrix M appearing in Eq. (14), as well as in Eq. (21), is defined as

$$M = \begin{bmatrix} & & \boldsymbol{m}_{17}^T & \boldsymbol{m}_{18}^T \\ & & \boldsymbol{m}_{27}^T & \boldsymbol{m}_{28}^T \\ & \bar{M}_0 & \boldsymbol{m}_{37}^T & \boldsymbol{m}_{38}^T \\ & & \boldsymbol{m}_{47}^T & \boldsymbol{m}_{48}^T + \boldsymbol{b}_1^T \\ & & \boldsymbol{m}_{57}^T + \boldsymbol{b}_2^T & \boldsymbol{m}_{58}^T \\ & & \boldsymbol{m}_{67}^T & \boldsymbol{m}_{68}^T \\ \boldsymbol{m}_{17}, \ldots, \boldsymbol{m}_{67} & & m_{77} & \boldsymbol{m}_{78}^T \\ \boldsymbol{m}_{18}, \ldots, \boldsymbol{m}_{68} & & m_{78} & m_{88} \end{bmatrix} \tag{A1}$$

with

$$\bar{M}_0 = \begin{bmatrix} m_t & 0 & -S_{tx} & a_1 & a_2 & -S_3 s_3 \\ 0 & m_t & -S_{ty} & a_3 & a_4 & S_3 c_3 \\ -S_{tx} & -S_{ty} & I_{t0} & a_5 & a_6 & S_3 L_0 s_{30} \\ a_1 & a_3 & a_5 & \bar{I}_1 & a_7 & a_8 \\ a_2 & a_4 & a_6 & a_7 & \bar{I}_2 & a_9 \\ -S_3 s_3 & S_3 c_3 & S_3 L_0 s_{30} & a_8 & a_9 & I_3 \end{bmatrix} \tag{A2}$$

in which

$$a_1 = -S_{t1}s_1 - \bar{\Phi}_{t1}^T\xi_1 c_1, \qquad a_2 = -S_{t2}s_2 - \bar{\Phi}_{t2}^T\xi_2 c_2$$

$$a_3 = S_{t1}c_1 - \bar{\Phi}_{t1}^T\xi_1 s_1, \qquad a_4 = S_{t2}c_2 - \bar{\Phi}_{t2}^T\xi_2 s_2$$

$$a_5 = S_{t1}L_0 s_{10} + \bar{\Phi}_{t1}^T\xi_1 L_0 c_{10}, \qquad a_6 = S_{t2}L_0 s_{20} + \bar{\Phi}_{t2}^T\xi_2 L_0 c_{20}$$

$$a_7 = S_{t2}L_1 c_{21} + S_{t2}\Phi_{12}^T\xi_1 s_{21} - \bar{\Phi}_{t2}^T\xi_2 L_1 s_{21} + \bar{\Phi}_{t2}^T\xi_2\Phi_{12}^T\xi_1 c_{21} \tag{A3}$$

$$a_8 = S_3 L_1 c_{31} + S_3\Phi_{12}^T\xi_1 s_{31}, \qquad a_9 = S_3 L_2 c_{32} + S_3\Phi_{23}^T\xi_2 s_{32}$$

$$b_1 = \bar{\Phi}_{t2}\Phi_{12}^T\xi_1 s_{21}, \qquad b_2 = -\Phi_{12}\bar{\Phi}_{t2}^T\xi_2 s_{21}$$

$$\bar{I}_1 = I_{t1} + \xi_1^T m_{77}\xi_1, \qquad \bar{I}_2 = I_{t2} + \xi_2^T m_{88}\xi_2$$

and

$$m_{17} = -\tilde{\Phi}_{t1}s_1, \qquad m_{27} = \tilde{\Phi}_{t1}c_1, \qquad m_{37} = \tilde{\Phi}_{t1}L_0 s_{10}$$

$$m_{47} = \tilde{\Phi}_1 + (m_2 + m_3)L_1\Phi_{12}, \qquad m_{57} = S_{t2}\Phi_{12}c_{21}$$

$$m_{67} = S_3\Phi_{12}c_{31}$$

$$m_{18} = -\tilde{\Phi}_{t2}s_2, \qquad m_{28} = \tilde{\Phi}_{t2}c_2, \qquad m_{38} = \tilde{\Phi}_{12}c_{21}$$

$$m_{67} = S_3\Phi_{12}c_{31} \tag{A4}$$

$$m_{48} = \tilde{\Phi}_{t2}L_1 c_{21}, \qquad m_{58} = \tilde{\Phi}_2 + m_3 L_2\Phi_{23}$$

$$m_{68} = S_3\Phi_{23}c_{32}$$

$$m_{77} = \Lambda_1 + (m_2 + m_3)\Phi_{12}\Phi_{12}^T, \qquad m_{78} = \Phi_{12}\bar{\Phi}_{t2}^T c_{21}$$

$$m_{88} = \Lambda_2 + m_3\Phi_{23}\Phi_{23}^T$$

and we note that $s_i = \sin\theta_i$, $c_i = \cos\theta_i$, $s_{ij} = \sin(\theta_i - \theta_j)$, and $c_{ij} = \cos(\theta_i - \theta_j)$. Moreover, we have used the following definitions:

$$m_t = m_0 + m_1 + m_2 + m_3$$

$$S_{tx} = S_{0x}\sin\theta_0 + S_{0y}\cos\theta_0 + (m_1 + m_2 + m_3)L_0\cos\theta_0$$

$$S_{ty} = -S_{0x}\cos\theta_0 + S_{0y}\sin\theta_0 + (m_1 + m_2 + m_3)L_0\sin\theta_0$$

$$S_{t1} = S_1 + (m_2 + m_3)L_1, \qquad S_{t2} = S_2 + m_3 L_2 \tag{A5}$$

$$I_{t0} = I_{0x} + I_{0y} + (m_1 + m_2 + m_3)L_0^2$$

$$I_{t1} = I_1 + (m_2 + m_3)L_1^2, \qquad I_{t2} = I_2 + m_3 L_2^2$$

$$\bar{\Phi}_{t1} = \tilde{\Phi}_1 + (m_2 + m_3)\Phi_{12}, \qquad \bar{\Phi}_{t2} = \tilde{\Phi}_2 + m_3\Phi_{23}$$

in which

$$m_i = \int_{\text{body}\,i}\rho_i\,\mathrm{d}D_i, \qquad i = 0, 1, 2, 3$$

$$S_i = \int_{\text{body}\,i}\rho_i x_i\,\mathrm{d}D_i, \qquad I_i = \int_{\text{body}\,i}\rho_i x_i^2\,\mathrm{d}D_i, \qquad i = 1, 2, 3$$

$$S_{0x} = \int_{\text{body}\,0}\rho_0 x\,\mathrm{d}D_0, \qquad S_{0y} = \int_{\text{body}\,0}\rho_0 y\,\mathrm{d}D_0$$

$$I_{0x} = \int_{\text{body}\,0}\rho_0 x^2\,\mathrm{d}D_0, \qquad I_{0y} = \int_{\text{body}\,0}\rho_0 y^2\,\mathrm{d}D_0 \tag{A6}$$

$$\tilde{\Phi}_i = \int_{\text{body}\,i}\rho_i\Phi_i\,\mathrm{d}D_i, \qquad \tilde{\Phi}_i = \int_{\text{body}\,i}\rho_i x_i\Phi_i\,\mathrm{d}D_i$$

$$\Lambda_i = \int_{\text{body}\,i}\rho_i\Phi_i\Phi_i^T\,\mathrm{d}D_i, \qquad i = 1, 2$$

$$\Phi_{12} = \Phi_1(x_1)|_{x_1 = L_1}, \qquad \Phi_{23} = \Phi_2(x_2)|_{x_2 = L_2}$$

The matrix G in Eq. (19) is defined as

$$G = \begin{bmatrix} 1 & 0 & 0 & 0 & 0 & 0 & \mathbf{0}^T & \mathbf{0}^T \\ 0 & 1 & 0 & 0 & 0 & 0 & \mathbf{0}^T & \mathbf{0}^T \\ 0 & 0 & 1 & -1 & 0 & 0 & \mathbf{0}^T & \mathbf{0}^T \\ 0 & 0 & 0 & 1 & -1 & 0 & \mathbf{0}^T & \mathbf{0}^T \\ 0 & 0 & 0 & 0 & 1 & -1 & \mathbf{0}^T & \mathbf{0}^T \\ 0 & 0 & 0 & 0 & 0 & 1 & \mathbf{0}^T & \mathbf{0}^T \\ \mathbf{0} & \mathbf{0} & \mathbf{0} & \mathbf{0} & -\Phi_1'(L_1) & \mathbf{0} & G_1 & 0 \\ \mathbf{0} & \mathbf{0} & \mathbf{0} & \mathbf{0} & \mathbf{0} & -\Phi_2'(L_2) & 0 & G_2 \end{bmatrix} \tag{A7}$$

where primes denote spatial derivatives and

$$G_i = [\Phi_i''(x_{i1})\cdots\Phi_i''(x_{im})], \qquad i = 1, 2 \tag{A8}$$

in which m is the number of actuators on each link. Here m is equal to the number of modes and G_i are square matrices.

The coefficient matrix C in Eq. (21) is defined as

$$C = \begin{bmatrix} 0 & 0 & C_{13} & C_{14} & C_{15} & C_{16} & C_{17} & C_{18} \\ 0 & 0 & C_{23} & C_{24} & C_{25} & C_{26} & C_{27} & C_{28} \\ 0 & 0 & 0 & C_{34} & C_{35} & C_{36} & C_{37} & C_{38} \\ 0 & 0 & C_{43} & 0 & C_{45} & C_{46} & C_{47} & C_{48} \\ 0 & 0 & C_{53} & C_{54} & 0 & C_{56} & C_{57} & C_{58} \\ 0 & 0 & C_{63} & C_{64} & C_{65} & 0 & C_{67} & C_{68} \\ \mathbf{0} & \mathbf{0} & C_{73} & C_{74} & C_{75} & C_{76} & 0 & C_{78} \\ \mathbf{0} & \mathbf{0} & C_{83} & C_{84} & C_{85} & C_{86} & C_{87} & 0 \end{bmatrix} \tag{A9}$$

where

$$C_{13} = S_{ty}\dot{\theta}_0, \qquad C_{14} = \left(-S_{t1}c_1 + \bar{\Phi}_{t1}^T\xi_1 s_1\right)\dot{\theta}_1$$

$$C_{15} = \left(-S_{t2}c_2 + \bar{\Phi}_{t2}^T\xi_2 s_2\right), \dot{\theta}_2 \qquad C_{16} = -S_3 c_3\dot{\theta}_3$$

$$C_{17} = -2\bar{\Phi}_{t1}^T c_1\dot{\theta}_1, \qquad C_{18} = -2\bar{\Phi}_{t2}^T c_2\dot{\theta}_2$$

$$C_{23} = -S_{tx}\dot{\theta}_0 \qquad C_{24} = \left(-S_{t1}s_1 - \bar{\Phi}_{t1}^T\xi_1 c_1\right)\dot{\theta}_1$$

$$C_{25} = \left(-S_{t2}s_2 - \bar{\Phi}_{t2}^T\xi_2 c_2\right)\dot{\theta}_2, \qquad C_{26} = -S_3 s_3\dot{\theta}_3$$

$$C_{27} = -2\bar{\Phi}_{t1}^T s_1\dot{\theta}_1, \qquad C_{28} = -2\bar{\Phi}_{t2}^T s_2\dot{\theta}_2$$

$$C_{34} = \left(S_{t1}L_0 c_{10} - \bar{\Phi}_{t1}^T\xi_1 L_0 s_{10}\right)\dot{\theta}_1,$$

$$C_{35} = \left(S_{t2}L_0 c_{20} - \bar{\Phi}_{t2}^T\xi_2 L_0 s_{20}\right)\dot{\theta}_2$$

$$C_{36} = S_3 L_0 c_{30}\dot{\theta}_3, \qquad C_{37} = 2\bar{\Phi}_{t1}^T L_0 c_{10}\dot{\theta}_1$$

$$C_{38} = 2.0\bar{\Phi}_{t2}^T L_0 c_{20}\dot{\theta}_2$$

$$C_{43} = \left(-S_{t1}L_0 c_{10} + \bar{\Phi}_{t1}^T\xi_1 L_0 s_{10}\right)\dot{\theta}_0$$

$$C_{45} = \left(-S_{t2}L_1 s_{21} - \bar{\Phi}_{t2}^T\xi_2 L_1 c_{21} + S_{t2}\Phi_{12}^T\xi_1 c_{21} - \bar{\Phi}_{t2}^T\xi_2\Phi_{12}^T\xi_1 s_{21}\right)\dot{\theta}_2$$

$$C_{46} = \left(-S_3 L_1 s_{31} + S_3\Phi_{12}^T\xi_1 c_{31}\right)\dot{\theta}_3$$

$$C_{47} = 2\xi_1^T\left(\Lambda_1 + (m_2 + m_3)\Phi_{12}\Phi_{12}^T\right)\dot{\theta}_1$$

$$C_{48} = 2\left(-L_1 s_{21}\bar{\Phi}_{t2}^T + \Phi_{12}^T\xi_1 c_{21}\bar{\Phi}_{t2}^T\right)\dot{\theta}_2 \tag{A10}$$

$$C_{53} = \left(-S_{t2}L_0 c_{20} + \bar{\Phi}_{t2}^T\xi_2 L_0 s_{20}\right)\dot{\theta}_0$$

$$C_{54} = \left(S_{t2}L_1 s_{21} + \bar{\Phi}_{t2}^T \xi_2 L_1 c_{21} - S_{t2}\Phi_{12}^T \xi_1 c_{21} + \bar{\Phi}_{t2}^T \xi_2 \Phi_{12}^T \xi_1 s_{21}\right)\dot{\theta}_1$$

$$C_{56} = \left(-S_3 L_2 s_{32} + S_3 \Phi_{23}^T \xi_2 c_{32}\right)\dot{\theta}_3,$$

$$C_{57} = 2\left(S_{t2}s_{21}\Phi_{12}^T + \bar{\Phi}_{t2}^T \xi_2 c_{21}\Phi_{12}^T\right)\dot{\theta}_1$$

$$C_{58} = 2\xi_2^T\left(\Lambda_2 + m_3\Phi_{23}\Phi_{23}^T\right)\dot{\theta}_1, \qquad C_{63} = -S_3 L_0 c_{30}\dot{\theta}_0$$

$$C_{64} = \left(S_3 L_1 s_{31} - S_3 \Phi_{12}^T \xi_1 c_{31}\right)\dot{\theta}_1$$

$$C_{65} = \left(S_3 L_2 s_{32} - S_3 \Phi_{23}^T \xi_2 c_{32}\right)\dot{\theta}_2, \qquad C_{67} = 2S_3 s_{31}\Phi_{23}^T\dot{\theta}_2$$

$$C_{68} = 2S_3 s_{32}\Phi_{23}^T\dot{\theta}_2, \qquad C_{73} = -\bar{\Phi}_{t1}L_0 c_{10}\dot{\theta}_0$$

$$C_{74} = -\left[\Lambda_1 + (m_2+m_3)\Phi_{12}\Phi_{12}^T\right]\xi_1\dot{\theta}_1$$

$$C_{75} = \left(-S_{t2}s_{21}\Phi_{12} - \bar{\Phi}_{t2}^T \xi_2 c_{21}\Phi_{12}\right)\dot{\theta}_2$$

$$C_{76} = -S_3 s_{31}\Phi_{12}\dot{\theta}_3, \qquad C_{78} = -2\Phi_{12}\bar{\Phi}_{t2}^T s_{21}\dot{\theta}_2$$

$$C_{83} = -\bar{\Phi}_{t2}L_0 c_{20}\dot{\theta}_0, \qquad C_{84} = \left(L_1 s_{21}\bar{\Phi}_{t2} - \Phi_{12}^T \xi_1 c_{21}\bar{\Phi}_{t2}\right)\dot{\theta}_1$$

$$C_{85} = -\left(\Lambda_2 + m_3\Phi_{23}\Phi_{23}^T\right)\xi_2\dot{\theta}_2, \qquad C_{86} = -S_3 s_{32}\Phi_{23}\dot{\theta}_3$$

$$C_{87} = 2\bar{\Phi}_{t2}\Phi_{12}^T s_{21}\dot{\theta}_1$$

Appendix B: Matrices in Partitioned Equations of Motion

The mass matrix M_r and the coefficient matrix C_r in Eq. (23) are defined as

$$M_r = \begin{bmatrix} m_t & 0 & -S_{tx} & -S_{t1}s_1 & -S_{t2}s_2 & -S_3 s_3 \\ 0 & m_t & -S_{ty} & S_{t1}c_1 & S_{t2}c_2 & S_3 c_3 \\ -S_{tx} & -S_{ty} & I_{t0} & S_{t1}L_0 s_{10} & S_{t2}L_0 s_{20} & S_3 L_0 s_{30} \\ -S_{t1}s_1 & S_{t1}c_1 & S_{t1}L_0 s_{10} & I_{t1} & S_{t2}L_1 c_{21} & S_3 L_1 c_{31} \\ -S_{t2}s_2 & S_{t2}c_2 & S_{t2}L_0 s_{20} & S_{t2}L_1 c_{21} & I_{t2} & S_3 L_2 c_{32} \\ -S_3 s_3 & S_3 c_3 & S_3 L_0 s_{30} & S_3 L_1 c_{31} & S_3 L_2 c_{32} & I_3 \end{bmatrix} \tag{B1}$$

$$C_r = \begin{bmatrix} 0 & 0 & S_{ty}\dot{\theta}_0 & -S_{t1}c_1\dot{\theta}_1 & -S_{t2}c_2\dot{\theta}_2 & -S_3 c_3\dot{\theta}_3 \\ 0 & 0 & -S_{tx}\dot{\theta}_0 & -S_{t1}s_1\dot{\theta}_1 & -S_{t2}s_2\dot{\theta}_2 & -S_3 s_3\dot{\theta}_3 \\ 0 & 0 & 0 & S_{t1}L_0 c_{10}\dot{\theta}_1 & S_{t2}L_0 c_{20}\dot{\theta}_2 & S_3 L_0 c_{30}\dot{\theta}_3 \\ 0 & 0 & -S_{t1}L_0 c_{10}\dot{\theta}_0 & 0 & -S_{t2}L_1 s_{21}\dot{\theta}_2 & -S_3 L_1 s_{31}\dot{\theta}_3 \\ 0 & 0 & -S_{t2}L_0 c_{20}\dot{\theta}_0 & S_{t2}L_1 s_{21}\dot{\theta}_1 & 0 & -S_3 L_2 s_{32}\dot{\theta}_3 \\ 0 & 0 & -S_3 L_0 c_{30}\dot{\theta}_0 & S_3 L_1 s_{31}\dot{\theta}_1 & S_3 L_2 s_{32}\dot{\theta}_2 & 0 \end{bmatrix} \tag{B2}$$

The disturbance vector $\boldsymbol{d}_e$ in Eq. (23) is defined as

$$\boldsymbol{d}_e = M_{re}\ddot{\boldsymbol{q}}_e + C_{re}\dot{\boldsymbol{q}}_e + \left(K_M^e + K_C^e\right)\boldsymbol{q}_e \tag{B3}$$

where

$$M_{re} = \begin{bmatrix} \boldsymbol{m}_{17} & \boldsymbol{m}_{18} \\ \boldsymbol{m}_{27} & \boldsymbol{m}_{28} \\ \vdots & \vdots \\ \boldsymbol{m}_{67} & \boldsymbol{m}_{68} \end{bmatrix} \tag{B4}$$

$$C_{re} = \begin{bmatrix} -2\bar{\Phi}_{t1}^T c_1\dot{\theta}_1 & -2\bar{\Phi}_{t2}^T c_2\dot{\theta}_2 \\ -2\bar{\Phi}_{t1}^T s_1\dot{\theta}_1 & -2\bar{\Phi}_{t2}^T s_2\dot{\theta}_2 \\ 2\bar{\Phi}_{t1}^T L_0 c_{10}\dot{\theta}_1 & 2\bar{\Phi}_{t2}^T L_0 c_{20}\dot{\theta}_2 \\ 0 & -2\bar{\Phi}_{t2}^T L_1 s_{21}\dot{\theta}_2 \\ 2\Phi_{12}^T S_{t2}s_{21}\dot{\theta}_1 & 0 \\ 2\Phi_{12}^T S_3 s_{31}\dot{\theta}_1 & 2\Phi_{23}^T S_3 s_{32}\dot{\theta}_2 \end{bmatrix} \tag{B5}$$

Moreover,

$$K_M^e = \begin{bmatrix} -\bar{\Phi}_{t1}^T c_1\ddot{\theta}_1 & -\bar{\Phi}_{t2}^T c_2\ddot{\theta}_2 \\ -\bar{\Phi}_{t1}^T s_1\ddot{\theta}_1 & -\bar{\Phi}_{t2}^T s_2\ddot{\theta}_2 \\ \bar{\Phi}_{t1}^T L_0 c_{10}\ddot{\theta}_1 & \bar{\Phi}_{t2}^T L_0 c_{20}\ddot{\theta}_2 \\ \boldsymbol{k}_{M1} & -\bar{\Phi}_{t2}^T L_1 s_{21}\ddot{\theta}_2 \\ \Phi_{12}^T S_{t2}s_{21}\ddot{\theta}_1 & \boldsymbol{k}_{M2} \\ \Phi_{12}^T S_3 s_{31}\ddot{\theta}_1 & \Phi_{23}^T S_3 s_{32}\ddot{\theta}_2 \end{bmatrix} \tag{B6}$$

in which

$$\boldsymbol{k}_{M1} = -\bar{\Phi}_{t1}^T(c_1\ddot{x}_0 + s_1\ddot{y}_0 - L_0 c_{10}\ddot{\theta}_0) + \Phi_{12}^T(S_{t2}s_{21}\ddot{\theta}_2 + S_3 s_{31}\ddot{\theta}_3)$$

$$\boldsymbol{k}_{M2} = -\bar{\Phi}_{t2}^T(c_2\ddot{x}_0 + s_2\ddot{y}_0 - L_0 c_{20}\ddot{\theta}_0) - \bar{\Phi}_{t2}^T L_1 s_{21}\ddot{\theta}_1 + \Phi_{23}S_3 s_{32}\ddot{\theta}_3 \tag{B7}$$

and

$$K_C^e = \begin{bmatrix} \bar{\Phi}_{t1}^T s_1\dot{\theta}_1^2 & \bar{\Phi}_{t2}^T s_2\dot{\theta}_2^2 \\ -\bar{\Phi}_{t1}^T c_1\dot{\theta}_1^2 & -\bar{\Phi}_{t2}^T c_2\dot{\theta}_2^2 \\ -\bar{\Phi}_{t1}^T L_0 s_{10}\dot{\theta}_1^2 & -\bar{\Phi}_{t2}^T L_0 s_{20}\dot{\theta}_2^2 \\ \boldsymbol{k}_{C1} & -\bar{\Phi}_{t2}^T L_1 c_{21}\dot{\theta}_2^2 \\ -\Phi_{12}^T S_{t2}c_{21}\dot{\theta}_1^2 & \boldsymbol{k}_{C2} \\ -\Phi_{12}^T S_3 c_{31}\dot{\theta}_1^2 & -\Phi_{23}^T S_3 c_{32}\dot{\theta}_2^2 \end{bmatrix} \tag{B8}$$

in which

$$\boldsymbol{k}_{C1} = \bar{\Phi}_{t1}^T L_0 s_{10}\dot{\theta}_0^2 + \Phi_{12}^T S_{t2}c_{21}\dot{\theta}_2^2 + \Phi_{12}^T S_3 c_{31}\dot{\theta}_3^2$$

$$\boldsymbol{k}_{C2} = \bar{\Phi}_{t2}^T L_0 s_{20}\dot{\theta}_0^2 + \bar{\Phi}_{t2}^T L_1 c_{21}\dot{\theta}_1^2 + \Phi_{23}^T S_3 c_{32}\dot{\theta}_3^2 \tag{B9}$$

The mass matrix M_e and the coefficient matrix C_e are defined as

$$M_e = \begin{bmatrix} \Lambda_1 + (m_2+m_3)\Phi_{12}\Phi_{12}^T & \Phi_{12}\bar{\Phi}_{t2}^T c_{21} \\ \bar{\Phi}_{t2}\Phi_{12}^T c_{21} & \Lambda_2 + m_3\Phi_{23}\Phi_{23}^T \end{bmatrix} \tag{B10}$$

$$C_e = \begin{bmatrix} 0 & -2\Phi_{12}\bar{\Phi}_{t2}^T s_{21}\dot{\theta}_2 \\ 2\bar{\Phi}_{t2}\Phi_{12}^T s_{21}\dot{\theta}_1 & 0 \end{bmatrix} \tag{B11}$$

and the coefficient matrix K_e is defined as

$$K_e = K + K_M + K_C \tag{B12}$$

where

$$K = \begin{bmatrix} \bar{K}_1 & 0 \\ 0 & \bar{K}_2 \end{bmatrix} \tag{B13}$$

$$K_M = \begin{bmatrix} 0 & -\Phi_{12}\bar{\Phi}_{t2}^T s_{21}\ddot{\theta}_2 \\ \bar{\Phi}_{t2}\Phi_{12}^T s_{21}\ddot{\theta}_1 & 0 \end{bmatrix} \tag{B14}$$

and

$$K_C = \begin{bmatrix} -\left(\Lambda_1 + (m_2+m_3)\Phi_{12}\Phi_{12}^T\right)\dot{\theta}_1^2 & -\Phi_{12}\bar{\Phi}_{t2}^T c_{21}\dot{\theta}_2^2 \\ -\bar{\Phi}_{t2}\Phi_{12}^T c_{21}\dot{\theta}_1^2 & -\left(\Lambda_2 + m_3\Phi_{23}\Phi_{23}^T\right)\dot{\theta}_2^2 \end{bmatrix} \tag{B15}$$

The disturbance vector $\boldsymbol{d}_r$ is defined as

$$\boldsymbol{d}_r = M_{re}^T \ddot{\boldsymbol{q}}_r + C_{er}\dot{\boldsymbol{q}}_r \tag{B16}$$

where M_{re} is given by Eq. (B4) and

$$C_{er} = \begin{bmatrix} 0 & 0 & -\bar{\Phi}_{t1} L_0 c_{10}\dot{\theta}_0 & 0 & -\Phi_{12} S_{t2} s_{21}\dot{\theta}_2 & -\Phi_{12} S_3 s_{31}\dot{\theta}_3 \\ 0 & 0 & -\bar{\Phi}_{t2} L_0 c_{20}\dot{\theta}_0 & \bar{\Phi}_{t2} L_1 s_{21}\dot{\theta}_1 & 0 & -\Phi_{23} S_3 s_{32}\dot{\theta}_3 \end{bmatrix} \tag{B17}$$

Acknowledgments

This work was supported by the Air Force Office of Scientific Research, Grant F49620-89-C-0045, monitored by Spencer T. Wu, and by NASA, Grant NAG-1-225, monitored by Raymond C. Montgomery.

References

[1]Longman, R. W., "The Kinetics and Workspace of a Satellite-Mounted Robot," *Journal of the Astronautical Sciences*, Vol. 38, No. 4, 1990, pp. 423–439.

[2]Lindberg, R. E., Longman, R. W., and Zedd, M. F., "Kinematic and Dynamics Properties of an Elbow Manipulator Mounted on a Satellite," *Journal of the Astronautical Sciences*, Vol. 38, No. 4, 1990, pp. 397–421.

[3]Vafa, Z., and Dubowsky, S., "On the Dynamics of Space Manipulators Using the Virtual Manipulator, with Applications to Path Planning," *Journal of the Astronautical Sciences*, Vol. 38, No. 4, 1990, pp. 441–472.

[4]Alexander, H. L., and Cannon, R. H., "An Extended Operational-Space Control Algorithm for Satellite Manipulators," *Journal of the Astronautical Sciences*, Vol. 38, No. 4, 1990, pp. 473–486.

[5]Nenchev, D., Umetani, Y., and Yoshida, K., "Analysis of a Redundant Free-Flying Spacecraft/Manipulator System," *IEEE Transactions on Robotics and Automation*, Vol. 8, No. 1, 1992, pp. 1–6.

[6]Nakamura, Y., and Mukherjee, R., "Nonholonomic Path Planning via a Bidirectional Approach," *IEEE Transactions on Robotics and Automation*, Vol. 7, No. 4, 1991, pp. 500–514.

[7]Nakamura, Y., *Advanced Robotics: Redundancy and Optimization*, Addison–Wesley, Reading, MA, 1991.

[8]Wang, P. K. C., "Automatic Assembly of Space Station," *Proceedings of the Workshop on Identification and Control of Flexible Space Structures*, Vol. 1, 1985, pp. 67–101.

[9]Novakovic, Z. R., "Lyapunov-Like Methodology for Robot Tracking Control Synthesis," *International Journal of Control*, Vol. 51, No. 3, 1990, pp. 567–583.

[10]Meirovitch, L., and Quinn, R. D., "Equations of Motion for Maneuvering Flexible Spacecraft," *Journal of Guidance, Control, and Dynamics*, Vol. 10, No. 5, 1987, pp. 453–465.

[11]Meirovitch, L., and Quinn, R. D., "Maneuvering and Vibration Control of Flexible Spacecraft," *Journal of Astronautical Sciences*, Vol. 35, No. 2, 1987, pp. 301–328.

[12]Meirovitch, L., and Kwak, M. K., "Dynamics and Control of Spacecraft with Retargeting Flexible Antennas," *Journal of Guidance, Control, and Dynamics*, Vol. 13, No. 2, 1990, pp. 241–248.

[13]Meirovitch, L., and Kwak, M. K., "Control of Flexible Spacecraft with Time-Varying Configuration," *Journal of Guidance, Control, and Dynamics*, Vol. 15, No. 2, 1992, pp. 314–324.

[14]Modi, V. J., and Chang, J. K., "Performance of an Orbiting Flexible Mobile Manipulator," *Transactions of the ASME: Journal of Mechanical Design*, Vol. 113, 1991, pp. 516–524.

[15]Meirovitch, L., and Lim, S., "Maneuvering and Control of Flexible Space Robots," *Journal of Guidance, Control, and Dynamics*, Vol. 17, No. 3, 1994, pp. 520–528.

[16]Koivo, A. J., and Lee, K. S., "Self-Tuning Control of a Two-Link Manipulator with a Flexible Forearm," *International Journal of Robotics Research*, Vol. 11, No. 4, 1992, pp. 383–395.

[17]Bang, H., and Junkins, J. L., "Liapunov Optimal Control Laws for Flexible Structures Maneuver and Vibration Control," *Advances in the Astronautical Sciences*, Vol. 75, Pt. I, 1990, p. 563.

[18]Meirovitch, L., and Chen, Y., "Trajectory and Control Optimization for Flexible Space Robots," *Journal of Guidance, Control, and Dynamics*, Vol. 18, No. 3, 1995, pp. 493–502.

[19]Meirovitch, L., and Kwak, M. K., "Rayleigh–Ritz Based Substructure Synthesis for Flexible Multibody Systems," *AIAA Journal*, Vol. 19, No. 10, 1991, pp. 1709–1719.

[20]Anderson, B. D. O., "Adaptive Systems, Lack of Persistency of Excitation and Bursting Phenomena," *Automatica*, Vol. 21, No. 3, 1985, pp. 247–258.

[21]Franklin, G. F., Powell, J. D., and Workman, M. L., *Digital Control of Dynamic Systems*, Addison–Wesley, New York, 1990.